



## Deriving Vertical Profiles of Aerosol Sizes from TES

M. Wolff (1), R. T. Clancy (1), M. Smith (2), T. McConnochie (3), D. Flittner (4), and T. Fouchet (5)

(1) Space Science Institute, Colorado, USA, (2) NASA/Goddard Space Flight Facility, Maryland, USA, (3) University of Maryland, Maryland, USA, (4) NASA/Langley Research Center, Virginia, USA, (5) Observatoire de Paris, Meudon, France  
(mjwolff@space-science.org)

### Abstract

Vertical variations in aerosol particle sizes can have a dramatic effect in their net impact on the state and evolution of the Martian atmosphere. Recent analyses of data from the Spectroscopy for the Investigation of the Characteristics of the Atmosphere of Mars (SPICAM; e.g., [1,2]) and the Thermal Emission Spectrometer (TES; [3,4]) instruments offer some long overdue progress in constraining this aspect of aerosols. However, significantly more work remains to be done along these lines in order to better constrain and inform modern dynamical simulations of the Martian atmosphere. Thus, the primary goal of our work is to perform retrievals of particle size as a function of altitude for both dust and water ice aerosols. The choice of the TES dataset, with pole-to-pole coverage over a period of nearly three martian years, provides the crucial systematic temporal and spatial sampling. Additional leverage on the particle size will be obtained by using both solarband bolometry and infrared (IR) spectroscopy. In this presentation, we provide some initial results of this work, focusing on the 2001 planet encircling dust event. In addition, we summarize (briefly) the results of our spherical radiative transfer validation exercises.

### 1. Radiative Transfer Background

The scarcity of previous efforts may be attributed, at least partially, to the dearth of applicable public-domain radiative transfer (RT) tools. This paucity is further emphasized by the continuing nature of the Mars Reconnaissance Orbiter mission, and in particular, the growing volume of Mars Climate Sounder limb observations. As a result, we felt it would be beneficial for the Mars community (and us as well) to develop an “exact,” efficient algorithm, and placing it in the public domain. Although this particular coding effort is limited to the IR regime, we are in the process of performing a series of

validation exercises for in the visible regime (using a fully spherical Monte Carlo (MC) algorithm, i.e., [5]) in order to explore the applicability of a particular approximation that has been employed in the visible regime (for both Martian and terrestrial applications), the so-called Plane-Parallel Source Function.

#### 1.1 Successive Orders of Scattering

In terms of this project, we were highly motivated to develop a new code by the computational cost of the MC RT, even in a 1-D mode. Because the IR regime benefits from the reduced complexity of the absence of a solar beam, the task is not as problematic as one might assume. Allowing oneself to consider only spherical shell geometry (i.e., 1-D in the radial coordinate), one can exploit azimuthal symmetry and apply the technique known as the Successive Orders of Scattering (SOS; e.g., [6,7]). Given that a public version of this code should be available by the time of our presentation, we dedicate some text here to a general description of the SOS approach.

The SOS method can be pictured as an expansion of the radiation field in terms of the number of scatterings that have occurred between the source and observer. In other words,  $I(s) = \sum_{i=0} I_i(s)$ , where  $s$  is the coordinate along the line of sight, and  $i=0$  represents emitted photons going directly to the observer, and  $1,2,3, \dots$  are the contributions from light scattered  $1,2,3, \dots$  times. Basically, the RT equation is solved repeatedly along a set of “tangent” rays through a spherical atmosphere. As can be seen in Figure 1, the properties of a given ray ( $S$ ) can be defined by the radius (or “impact parameter”,  $p$ ) of the tangent point as well as by the intersections of the ray with the radial mesh ( $r$ ) points exterior to the tangent radius. This schematic shows only one quadrant; the actual integration is performed along the ray between the two points at which it leaves the atmosphere. The bottom of the atmosphere is defined by the “core” or surface radius ( $r_c$ ). Within this

paradigm, it is a simple matter to integrate the standard RT equation for the desired number of scattering orders.

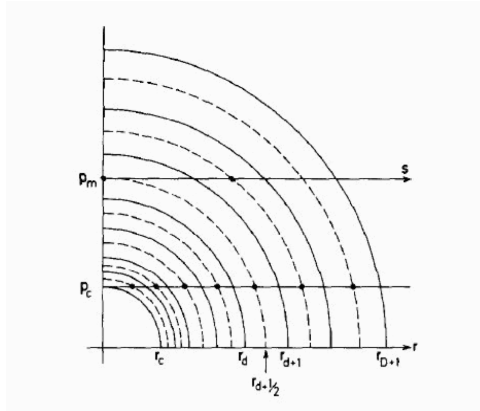


Figure 1: Schematic of our SOS radiative transfer mesh. RT is performed successively along each ray S. Each ray is defined with respect to the radial mesh point at the tangent point.

Starting with  $i = 0$ , the source function is that of Planck function and the integration along the tangent ray can be accomplished with a basic numerical integration; we use linear interpolation and a Gaussian quadrature. To add additional orders of scattering, the source function of the  $i$ -th order simply becomes an integral over solid angle of the previous order intensity ( $I(i-1)$ ). For each radial level ( $r_d$ ), the integral over solid angle is computed using the polar angle mesh defined by the intersection points of the tangent rays and  $r_d$ . Convergence is typically defined as when the order  $i$  falls below some predefined fraction of the total radiance.

Figure 2 provides two example calculations of our SOS implementation compared to those from the MC code for some generic Martian atmospheric conditions: a wavelength of  $10 \mu\text{m}$  and two optical depths. The MC error bars are approximately 2% of the radiance signal at lower tangent heights, reaching 4% near the “top” of the atmosphere. As an illustration of why we prefer using the SOS for the IR, each of the MC calculations represents about 1 hr on a single Intel 3 GHz processor, while the SOS calculations took 15 sec and 35 sec for the lower and higher optical depths, respectively. The CPU time associated with the SOS method could be reduced at

the potential expense of accuracy by employing fewer mesh points or a larger convergence cutoff; 0.001 was used in the figure, which required 4 and 7 orders of scattering, respectively. However, given that the speed of our SOS implementation is already comparable to that for a discrete-ordinates plane parallel code such as DISORT [8] (under the same atmospheric conditions), it is not clear that such a reduction in accuracy would be desirable. Instead, if needed, additional gains in efficiency can be made through parallelization. Such an effort would not be complicated given the natural discretization of the problem over wavelength and the relative simplicity with which such an implementation could be made using MPICH2.

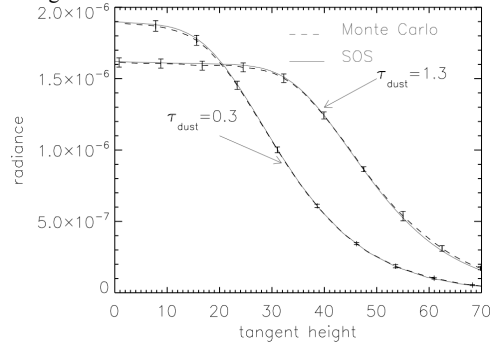


Figure 2: Results from our SOS implementation are compared to those from the Monte Carlo code. For simplicity, the dust is assumed to be uniformly mixed. The temperature profile is representative of conditions near the equator during southern summer.

## 1.2 Plane Parallel Source Function

A final algorithm to consider within the scope of our project involves the treatment of a spherical atmosphere by tracing a curved path in a plane-parallel representation. In this scenario, the attenuation of the incident and emergent beams are performed exactly for spherical geometry, but the multiple-scattering contribution (i.e., scattering source function) is implemented in plane-parallel geometry. In light of our SOS algorithm, there is no explicit need to consider such an approximation for the thermal regime. On the other hand, the computational intensity of the Monte Carlo calculation for the solar-band channel suggests a potential application if, and only if, the plane parallel source function (PPSF) approach can provide a sufficient level of accuracy.

Tests of the PPSF method (or an equivalent approximation) for optical wavelengths may be found in the terrestrial literature ([7], and references within). Although errors < 10% have been reported, the opacity sources in the test cases included a significant absorptive component. In addition, the dominant scattering mechanism is inherently isotropic (i.e., Rayleigh scattering). These conditions are not representative of the solarband regime in the Martian atmosphere. Clearly, a validation exercise containing a specific set of representative conditions would need to be carried out, using Monte Carlo results as “ground-truth.” In order to perform such a task, our experiments employ the PPSF codes developed by co-authors Smith and Fouchet. The solution method for these implementation is that of discrete ordinates, providing a full multiple-scattering treatment including both solar beam and thermal sources. If an acceptable accuracy can be realized with this technique for the solarband, even for a restricted range of aerosol loading conditions, the gain in computational efficiency would allow retrievals from a larger fraction of the TES limb database than would be possible using only the MC algorithm.

## 2. Retrieval Methodology

Our basic methodology is a synthesis of the iteration scheme employed by [9] for the TES IR observations with that from Clancy et al. where this combined approach alternates between the solarband and IR radiative transfer calculations. Fundamentally, we employ a set of nested iterations: an outer loop over  $r_{\text{eff}}$  and two interior loops that derive volume mixing ratios from the IR and solarband observations. Although our primary goal is particle size, the derivation of the volume mixing ratios for dust ( $q_{\text{dust}}$ ) and water ice ( $q_{\text{ice}}$ ) is a natural consequence of our quest for  $r_{\text{eff}}$ . When possible (e.g., warm surface nadir data are available), we derive the total optical depth and some measure of the  $r_{\text{eff}}$  in the lowest scale-height.

The size of the TES detector footprint and the instrumental point spread function restrict the effective vertical resolution to approximately 10 km (e.g., [10]). As such, there is little point in attempting to retrieve atmospheric parameters on a finer mesh. Following [9], we specify the parameters ( $r_{\text{eff}}, q$ ) at 10, 20, 30, 40, 50, and 60 km. The height of the top

level is essentially imposed by signal-to-noise while that of the lowest level by optical depth effects (a.k.a. “saturation”).

Although we are still in the “implementation” phase, our retrieval is being constructed to derive the parameter values at each level in the following way:

1. Select the appropriate temperature profile; surface emissivity, albedo, and temperature; and the transformation basis information for the specific TES observation. Determine initial guesses for  $r_{\text{eff}}$  and volume mixing ratios.
2. Extract the scattering properties from the aerosol database for current  $r_{\text{eff}}(z)$ .
3. With the IR limb spectra, use the nonlinear least squares fitting routine, MPFIT [11], and the SOS radiative transfer to calculate the “best fit” volume mixing ratios ( $q_i, q_d$ ) at six atmospheric levels for dust and water ice. The  $q$  values are converted to optical depth per unit length using the current aerosol properties. The model-data comparison is done after each model has been transformed to the new basis. The inherently higher vertical resolution of the model is degraded to match that of the TES data, i.e., 10 km.
4. Compute the solarband scattering properties using the relative contribution of dust and ice as determined by the  $q$  values of the previous step.
5. With the solarband limb data, use MPFIT and the MC (or PPSF) radiative transfer to calculate the “best-fit” total  $q$  for the same levels as Step 3. Decompose the mixing ratio into dust and water ice fractions using the weights of the previous step; calculate the individual optical depths per unit length.
6. Use the ratio of solarband-IR optical depths (solarband to  $9.3 \mu\text{m}$  for dust, solarband to  $12.1 \mu\text{m}$  for water ice) at each layer to produce new estimates for  $r_{\text{eff}}$  at each level by interpolating on the ratio of extinction cross sections in the aerosol model database.
7. Check for convergence in a given level and aerosol component by looking at the relative change in  $r_{\text{eff}}$  and the amplitude of  $q(\text{solarband})-q(\text{IR})$ . By definition, the actual  $r_{\text{eff}}$  should produce the same mixing ratios (within errors) for both the solarband and IR retrievals. In addition, one requires that for an

$r_{\text{eff}}$  at specific level to be considered converged, all the higher altitude levels must also have converged. This prevents a premature numerical convergence due to a serendipitous juxtaposition of values in the “higher” layers of the atmosphere.

8. Flag converged levels for each aerosol component to improve the computation efficiency, i.e., so that MPFIT no longer iterates on them. If all  $r_{\text{eff}}$  not converged, go to Step 2.

In the case that an appropriate set of nadir spectra are available with surface temperature above 220 K, the algorithm will attempt to constrain the total-column optical depth for each aerosol component as well as an estimate of the average  $r_{\text{eff}}$  below 10 km.

## 6. Current State and Plans for Actual Presentation

At the time abstract submission, we have completed basic development of the SOS algorithm. We are currently performing the numerical experiments described in Section 1.2 and as well as the integration of the individual pieces of software into the flow described Section 2. As a result, we intend to present at the meeting:

- 1) The summary of the Section 1.2 validation exercises
- 2) The initial results of the application of the entire retrieval scheme to the TES observations of the 2001 planet encircling dust event.
- 3) The plans for additional retrievals (aphelion cloud season, lower optical depth locations and seasons, etc.) and the distribution of the derived profiles.

## Acknowledgements

This work is (and has been) supported by NASA with a Mars Data Analysis Program award (grant NNX10AO23G) and an MRO Project contract to Malin Space Science Systems (JPL Contract 1275776).

## References

[1] Montmessin, F. et al.: Stellar occultations at UV wavelengths by the SPICAM instrument: Retrieval and

analysis of martian haze profiles. JGR 111, E09S09, 2006.

[2] Rannou, P. et al., Dust and cloud detection at the mars limb with UV scattered sunlight with SPICAM, JGR (Planets) 111, E09S10, 2006.

[3] Clancy, R. T., et al. Mars equatorial mesospheric clouds: Global occurrence and physical properties from Mars Global Surveyor Thermal Emission Spectrometer and Mars Orbiter Camera limb observations. JGR (Planets) 112 (E11), E04004, 2007.

[4] Clancy, R. T., et al.: Extension of atmospheric dust to high altitudes during the 2001 mars dust storm: MGS TES limb observations, Icarus, 207, 98, 2010.

[5] Wolff, M. et al: Constraints on dust aerosols from the Mars Exploration Rovers using MGS overflights and Mini- TES, JGR (Planets) 111 (E10), E12S17, 2006.

[6] Hansen, J. E., Travis, L. D.: Light scattering in planetary atmospheres, Space Science Reviews 16, 527–610, 1974.

[7] Bourassa, A. E., et al.: SASKTRAN: A spherical geometry radiative transfer code for efficient estimation of limb scattered sunlight, JQSRT 109, 52–73, 2008.

[8] Stamnes, K, et al.: Numerically stable algorithm for discrete ordinate-method radiative transfer in multiple scattering and emitting layered media, Applied Optics 27, 2502–2509, 1988.

[9] McConnochie, T. H., and Smith, M. D.: Three Martian Years of MGS-TES Aerosol Limb Sounding: Vertical Distributions, Diurnal Variations, and the Polar Night. AGU Fall Meeting, 2007.

[10] Conrath, B. J., et al.: Mars Global Surveyor Thermal Emission Spectrometer (TES) observations: Atmospheric temperatures during aerobraking and science phasing, JGR (Planets) 105, 9509–9520.

[11] Markwardt, C. B.: Non-Linear Least Squares Fitting in IDL with MPFIT," in proc. Astronomical Data Analysis Software and Systems XVIII, Quebec, Canada, ASP Conference Series, Vol. 411, eds. D. Bohlender, P. Dowler & D. Durand (Astronomical Society of the Pacific: San Francisco), p. 251-254, 2008.